Thermal Assessment and In-Situ Monitoring of Insulated Gate Bipolar Transistors in Power Electronic Modules

Preprint

Erick Gutierrez,[1] Kevin Lin,[1] Patrick McCluskey,[1] and Douglas DeVoto[2]

1 University of Maryland
2 National Renewable Energy Laboratory

Presented at ASME 2019 International Technical Conference and Exhibition on Packaging and Integration of Electronic and Photonic Microsystems (IPACK2019)
Anaheim, California
October 7–9, 2019

NREL is a national laboratory of the U.S. Department of Energy
Office of Energy Efficiency & Renewable Energy
Operated by the Alliance for Sustainable Energy, LLC

Conference Paper
NREL/CP-5400-73583
February 2020

Contract No. DE-AC36-08GO28308

Thermal Assessment and In-Situ Monitoring of Insulated Gate Bipolar Transistors in Power Electronic Modules

Preprint

Erick Gutierrez,[1] Kevin Lin,[1] Patrick McCluskey,[1] and Douglas DeVoto[2]

1 University of Maryland
2 National Renewable Energy Laboratory

Suggested Citation
Gutierrez, Erick, Kevin Lin, Patrick McCluskey, and Douglas DeVoto. 2020. *Thermal Assessment and In-Situ Monitoring of Insulated Gate Bipolar Transistors in Power Electronic Modules: Preprint*. Golden, CO: National Renewable Energy Laboratory. NREL/CP-5400-73583 https://www.nrel.gov/docs/fy20osti/73583.pdf.

NREL is a national laboratory of the U.S. Department of Energy
Office of Energy Efficiency & Renewable Energy
Operated by the Alliance for Sustainable Energy, LLC

This report is available at no cost from the National Renewable Energy Laboratory (NREL) at www.nrel.gov/publications.

Contract No. DE-AC36-08GO28308

Conference Paper
NREL/CP-5400-73583
February 2020

National Renewable Energy Laboratory
15013 Denver West Parkway
Golden, CO 80401
303-275-3000 • www.nrel.gov

THERMAL ASSESSMENT AND IN-SITU MONITORING OF INSULATED GATE BIPOLAR TRANSISTORS IN POWER ELECTRONIC MODULES

Erick Gutierrez, Kevin Lin, Patrick McCluskey
CALCE
Department of Mechanical Engineering
University of Maryland
College Park, MD, USA

Douglas DeVoto
National Renewable Energy Laboratory
Golden, CO, USA

ABSTRACT

Insulated gate bipolar transistor (IGBT) power modules are devices commonly used for switching of high voltages and currents. Usage and environmental conditions can cause these power modules to degrade over time, and this gradual process may eventually lead to catastrophic failure of the device. This degradation process may cause some early performance symptoms related to the state of health of the power module, making it possible to detect reliability degradation of the IGBT module. Testing can be used to accelerate this process, permitting a rapid determination of whether specific declines in device reliability can be characterized. In this study, thermal cycling was conducted on multiple power modules simultaneously in order to assess the effect of thermal cycling on the degradation of the power module. In-situ monitoring of temperature was performed from inside each power module using high temperature thermocouples. Device imaging and characterization were performed along with temperature data analysis, to assess failure modes and mechanisms within the power modules. While the experiment was aimed to assess the potential damage effects of thermal cycling on die attach, results indicated that wirebond degradation was the life limiting failure mechanism.

Keywords: Insulated Gate Bipolar Transistor (IGBT), Power Module, In-Situ Monitoring.

1. INTRODUCTION

Power electronic devices are used in a wide variety of applications requiring a range of load conditions from low to high power, including automotive propulsion, train traction, wind turbines, and solar inverters. A cross-section drawing of a typical power electronic module assembly is shown in FIGURE 1 [1]. The assembly often includes dice (i.e. IGBT chips), diodes, solder, substrates, wirebonds, a baseplate, thermal pads or grease, and a heatsink. It has been proposed that active condition monitoring of these power electronic modules can be used to predict and prevent failure before it occurs. On a more specific note, 34% of all power module systems fail due to failures of semiconductors or solders [2], so predicting failure by these failure mechanisms is of particular interest.

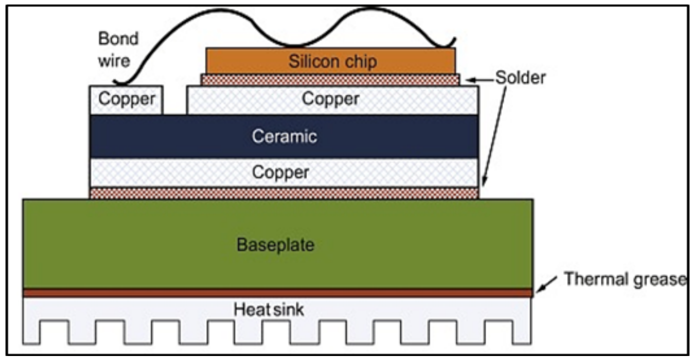

FIGURE 1: SCHEMATIC OF A TYPICAL POWER ELECTRONIC ASSEMBLY [1]

Insulated Gate Bipolar Transistors (IGBTs) are high-power switching devices, consisting of an n-channel MOSFET driving the gate of PNP bipolar junction transistor (BJT) (see Figure 2). The fast switching speed comes from the MOSFET, and the high current handling capability comes from the BJT. They, therefore, are able to operate at higher voltages and have higher current ratings compared to power MOSFETS [3].

Since IGBTs have suitable characteristics, they have become an ideal choice for power electronics applications (i.e. power converters, traction motor control) For this reason, it is important to understand the signals that can be monitored from a and IGBT module to determine system health, especially as related to the electrical and mechanical assembly integrity.

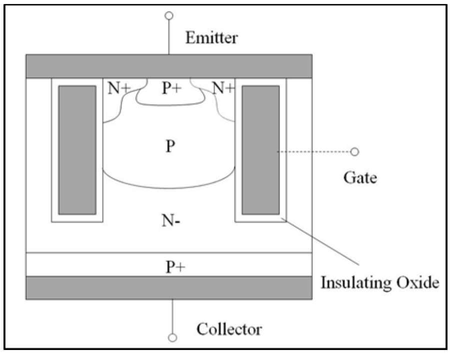

FIGURE 2: SCHEMATIC DIAGRAM SHOWING INTERNAL COMPONENTS OF AN IGBT.

Often, failures in power electronics components are the result of an induced stress from the operating conditions. There are two common methods by which the operating conditions induce stress that can limit module lifetime: thermal and power cycling [4], [5]. Power cycling induces load variations that typically create electrical failures, while thermal cycling induces temperature variations that create thermomechanical stress. In conventional uses, most power electronics systems undergo both forms of cycling, and as a result, experience both types of stresses [4], [6]. In many cases, power cycling can also be used to induce thermal cycling, as high currents through the IGBT modules will heat the junction, and thus create thermomechanical stress [7].

Common failure mechanisms of IGBT modules used in power converters include wirebond, substrate, and solder fatigue, which can cause changes in the electrical and thermal signals of the module. Some of these changes include increases of the collector-emitter voltage (V_{CE}) of a few percent, increases of the thermal resistance (R_{th}) from the IGBT junction to the case of up to 20%, and changes in gate oxide properties leading to an increase of the threshold gate voltage ($V_{GE(th)}$) [4]. These failure modes are hastened by operating at elevated temperatures [2].

The aim of this study was to investigate the use of these signals as possible methods for monitoring degradation of commercial off-the-shelf IGBT power modules during thermal cycling due to these failure mechanisms. In addition to monitoring the degradation of the IGBTs, the study also included offline inspection of devices that exhibited indications of failure to determine the potential failure mechanism responsible for the degradation. These inspections included data analysis and analytical device characterization. It was expected that data and image analysis would provide evidence to reveal failure mechanisms of devices that exhibit indicators of failure from thermal test data.

2. MATERIALS AND METHODS

The materials and methods utilized in this project involved the use of commercially available devices and experimental procedures used for accelerated life testing as described below.

2.1 Test Specimen

In order to perform the experiment, 12 commercial off-the-shelf (COTS) dual channel 1200V 450A power modules were used. Each power module comprised a total of 6 IGBTs and 6 corresponding diodes, encapsulated in a transparent silicone gel. An example of such a module (with the lid removed) is shown in Figure 3 for reference. Each power module was assembled with a heatsink and thermal pad to mimic a typical working configuration.

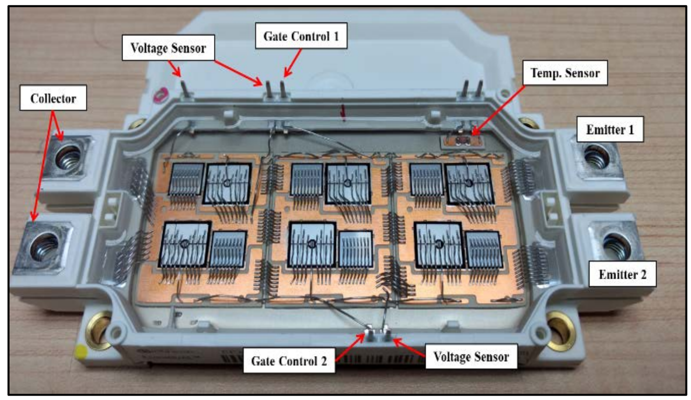

FIGURE 3: REPRESENTATIVE POWER MODULE USED DURING EXPERIMENT

2.2 Parameter Monitoring

In order to conduct condition monitoring during the experiment, a few parameters were selected to assess performance and degradation based on their sensitivity to degradation. The Junction Temperature parameter (T_J), is used due to the well-known correlation between temperature and degradation of IGBT. Similarly, the Collector-Emitter Voltage (V_{CE}) is also monitored due to its capability to detect die attach degradation [8]. Since the power modules were subjected to thermal cycling, it was expected that the test would cause fatigue on the solder and lead to fracture, cracking, or delamination. Damage in the solder attach would consequently affect the thermal path and cause an increase in T_J, and a change in electrical response (i.e. V_{CE}).

Two different approaches were examined for determining the junction temperature. First, the power module internal temperature sensor was used to collect data. The sensor outputs a voltage proportional to the substrate temperature, and that value is then converted to temperature in degrees Celsius. The other method involved a pre-calibrated Type-K thermocouple inserted through the protective layer of silicone gel on the IGBT power module. The thermocouple was mounted on the top surface of the chip and was connected to a data logger for temperature monitoring. The thermocouples used were calibrated at 0˚C and 100˚C respectively. According to the temperature profile in Figure 4, the thermocouple's temperature (shown in orange) was fairly consistent with the IGBT internal thermal diode (shown in blue) at room temperature, but it starts to deviate at temperatures above 80˚C and below -20˚C.

However, the thermocouple gives readings similar to the internal temperature sensor of the thermal chamber when set to a specific temperature. Since the thermocouple showed data readings closer to the thermal chamber sensor, it was used as the temperature reading during this research rather than the internal IGBT thermal diode.

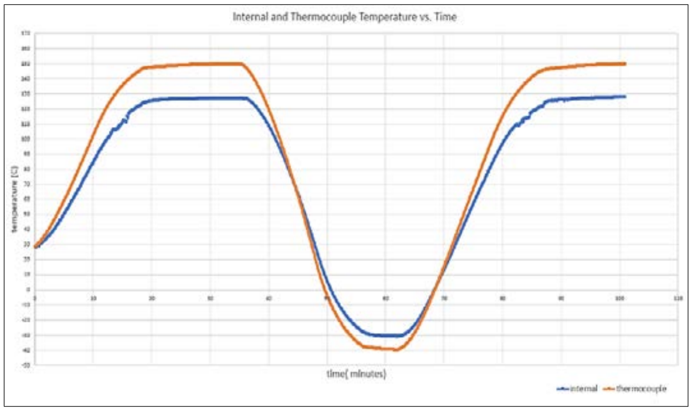

FIGURE 4: SAMPLE DATA OBTAINED DURING TEMPERATURE JUNCTION RECORDING - INTERNAL DIODE (BLUE) VS. INSERTED THERMOCOUPLE (ORANGE).

2.3 Thermal Cycling

In order to accelerate failure, thermal cycling was applied simultaneously to all 12 modules. The devices were placed together in a rack inside a temperature chamber. Figure 5 shows a photograph of the samples as placed and arranged inside the temperature chamber. A data logger was used to monitor the temperature of the modules during testing and the temperature chamber was programmed to thermally cycle the modules between -45ºC and 155ºC. The chamber uses an internal temperature sensor to verify that the interior is reaching the desired temperature. Liquid nitrogen was used during the cooling period in the thermal cycle and each cycle was of approximately one-hour duration.

FIGURE 5: SETUP OF POWER MODULES FOR SIMULTANEOUS THERMAL CYCLING.

2.4 Powering Specimen

After every 100 thermal cycles, the modules were taken from the thermal chamber and subjected to a powering assessment. This was done to observe any changes in the junction temperature resulting from a degradation in the thermal path due to the temperature cycling. In order to conduct this step, the same Type-K thermocouples used during thermal cycling were also used to monitor the temperature during powering assessment, while collector-emitter voltage (V_{CE}) was recorded at the same time. A power supply AEHR 20V 300A was used to power each individual module, and a datalogger was used to record the data. Each module was powered on individually for 2 minutes and then powered off until it cooled to room temperature (one channel at a time: A and B). The overall and individual setup for turning on the power modules can be observed in Figure 6 and Figure 7 below.

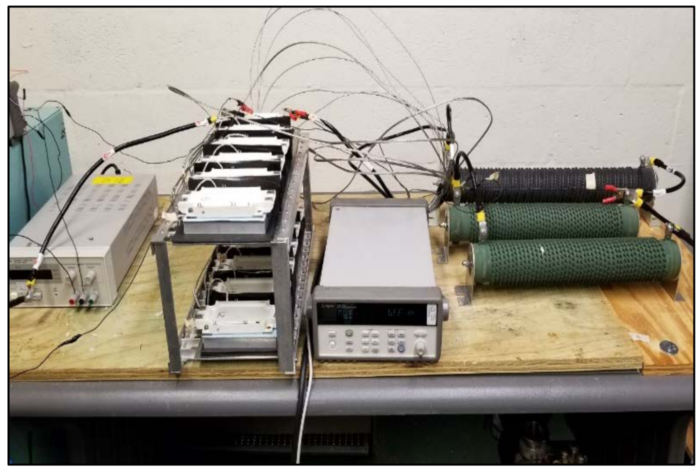

FIGURE 6: OVERALL SETUP FOR POWERING ON THE MODULES AFTER CONDUCTING THERMAL CYCLING

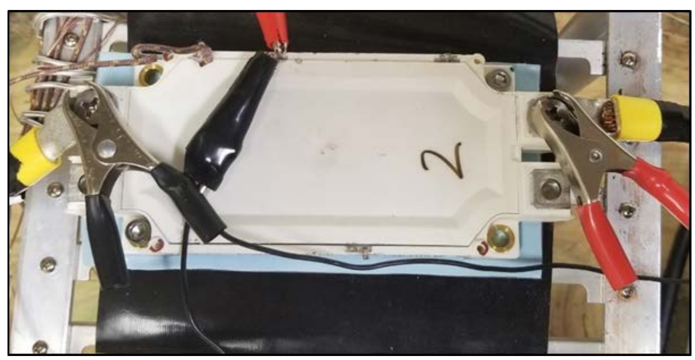

FIGURE 7: TOP VIEW OF INDIVIDUAL SETUP FOR A POWER MODULE USED FOR POWERING ON.

3. RESULTS AND DISCUSSION

3.1 Temperature and Electrical Response

The samples were exposed to a maximum of 1500 thermal cycles during the experiment. After every 100 thermal cycles, the modules were powered on, and the temperature recorded by the thermocouple was compared with all the other modules. One channel was powered first and then allowed to cool down prior to powering on the next channel on every module. The temperature response during the on state of the modules for channel A and B can be observed in Figure 8 and Figure 9, respectively. It is shown in Figure 8 that a bigger temperature deviation was observed for channel A (Blue) compared to channel B (Orange). More specifically, modules 1 and 4 showed a larger temperature deviation when the modules were powered on using channel A. The collector-emitter voltage (V_{CE}) suddenly increased after 600 thermal cycles (see Figure 10) but produced no significant increase in temperature (i.e. temperature remained low). This apparent failure contributed to the temperature deviation readings obtained from the datalogger when powering the modules on. This behavior was observed more clearly on modules 1 and 4, channel A respectively.

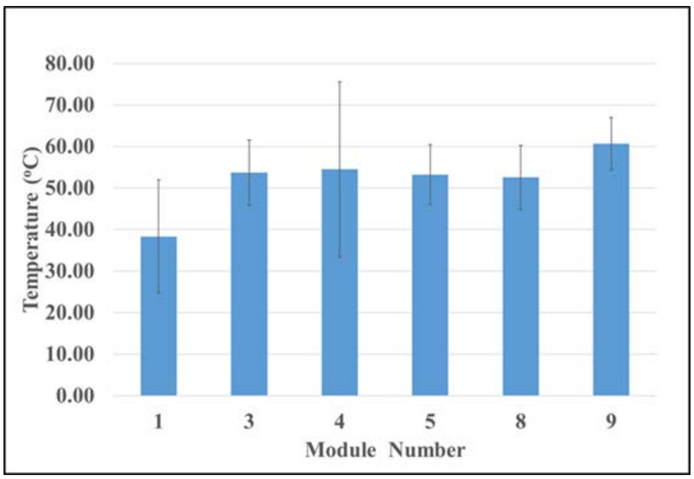

FIGURE 8: AVERAGE TEMPERATURE READINGS OBTAINED WHEN POWERING ON THE MODULES USING CHANNEL A.

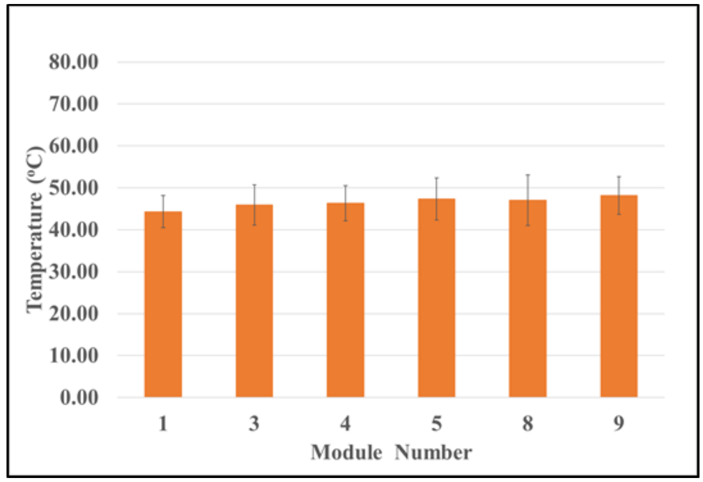

FIGURE 9: AVERAGE TEMPERATURE READINGS OBTAINED WHEN POWERING ON THE MODULES USING CHANNEL B.

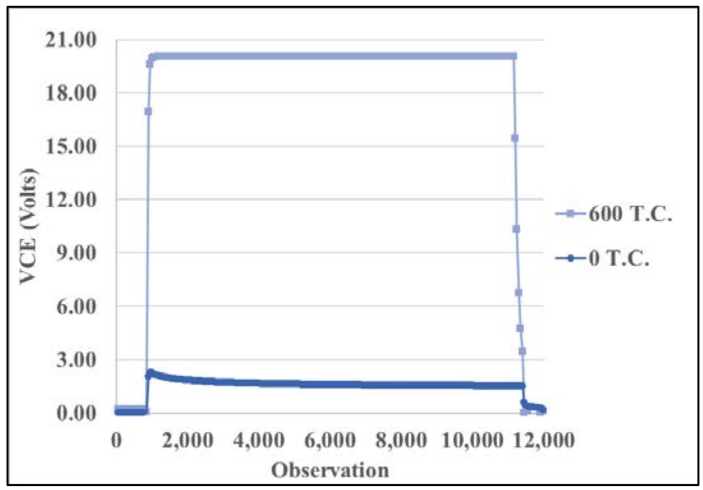

FIGURE 10: SAMPLE DATA OF V_{CE} RECORDED WHILE POWERING AT TWO DIFFERENT TIME PERIODS: PRIOR TO STARTING THERMAL CYCLING AND AFTER COMPLETING 600 THERMAL CYCLES (T.C.).

3.2 Device Inspection

The increase in the variation in this electrical parameter led to further characterization and inspection of the device for potential damage. All power modules were examined with a light optical microscope and inspected with x-rays to assess any potential damage in the device, particularly in the solder attach. While it was expected that an increase in temperature would be due to solder attach damage, this was not observed. X-ray imaging showed no evidence of cracks or delamination in the solder attach (see Figure 11). Some of the modules experienced a small oscillation of the V_{CE} and temperature throughout the test but did not fail within the 1500 cycles. The modules that did fail showed a similar oscillation in temperature and V_{CE} until a complete open circuit failure was observed as a spike in V_{CE} (see Figure 10). These failed samples were then opened for inspection and it was found that they failed by wirebond heel fracture (see Figure 12).

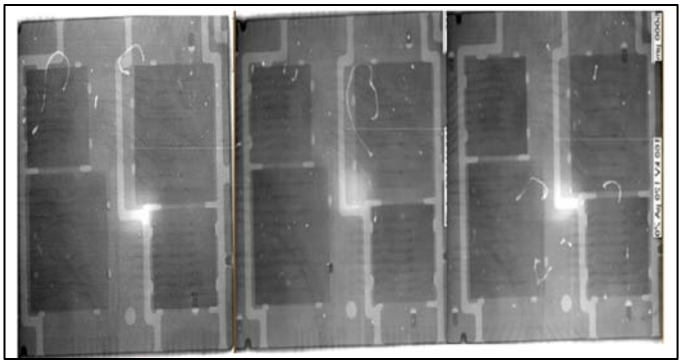

FIGURE 11: X-RAY IMAGING OF POWER MODULE WITH NO DAMAGE OBSERVED IN THE SOLDER ATTACH.

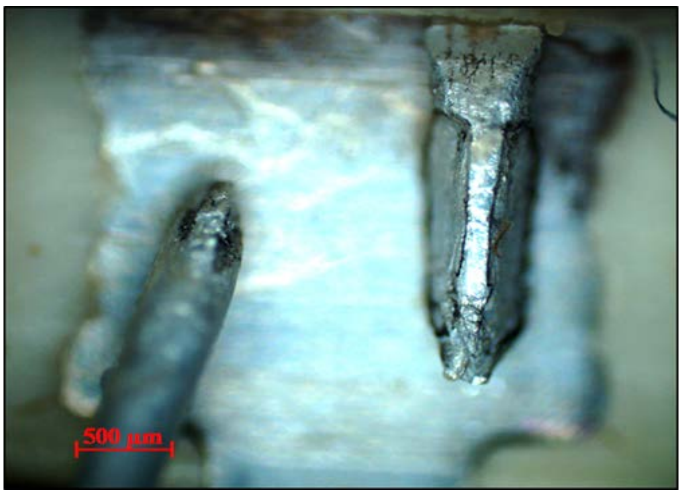

FIGURE 12: MICROSCOPE IMAGE OF A HEEL FRACTURE OBSERVED IN WIRBOND FROM POWER MODULE.

3.3 Wirebond Characterization

Since wirebonds were found to be damaged instead of solder attach, wirebond electrical characterization was performed in order to further investigate the modules, even though the present research was focused on solder damage. It is well known that thermal cycling can lead to damage on the wirebonds and flexural stresses due to this type of test can lead to fatigue failure [9]. Electrical characterization of each individual module was performed by running a gate-collector capacitance measurement using a B1505A curve tracer with ultra-high current expander UHC (See Figure 13). This type of characterization was chosen because previous studies had used it to identify potential damage of IGBTs by measuring the gate-collector capacitance with different frequencies [10]. The biggest difference observed between a new and a degraded device was found at 5 kHz, therefore the electrical characterization performed on the devices was done using this frequency for each gate in each module.

In order to minimize excess charge in each module, a 30-minute break was given between each measurement. A voltage sweep was applied from 0V to 30V using a 5 kHz frequency for measurement, however, the capacitance values did not change significantly with voltage, so the capacitances over all voltages were averaged to get the final value for each frequency measurement. Each module was setup in order to test one gate at a time, channel A and B, remove the module and setup the next one, until all the modules were measured before starting again with the next gate. The module setup can be observed in Figure 14 where the device is connected to the testing apparatus.

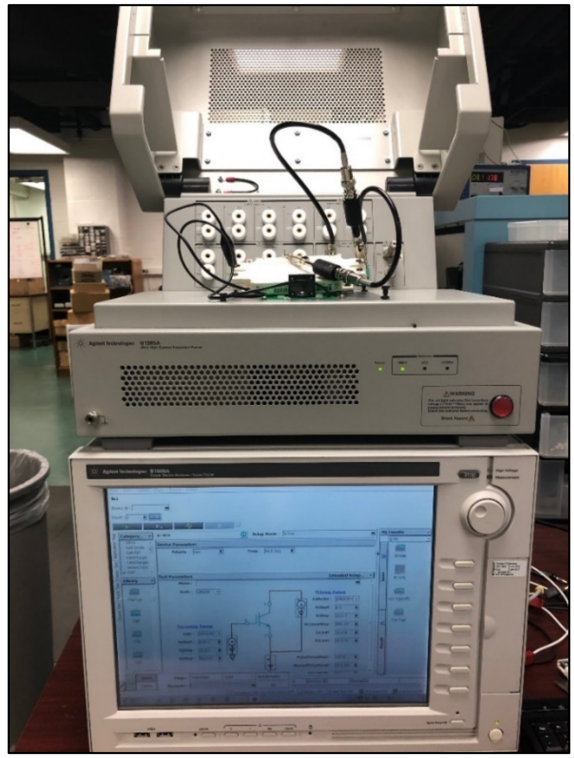

FIGURE 13: PICTURE TAKEN FROM THE FRONT SIDE OF THE B1505A CURVE TRACER WITH ULTRA HIGH CURRENT EXPANDER (UHC).

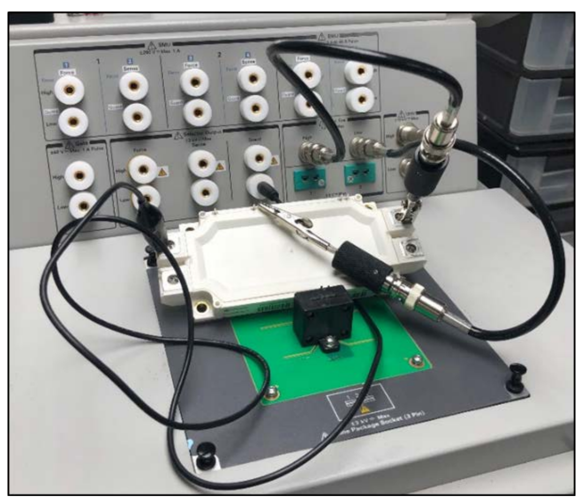

FIGURE 14: SETUP OF CURVE TRACER CONNECTED TO A POWER MODULE FOR ELECTRICAL CHARACTERIZATION.

The curve tracer was used to test each individual module to see any electrical variation on the device. Three fully operational power modules were tested to establish a baseline before testing the rest of the modules that went through thermal cycling. Some discrepancies were observed in the electrical behavior of some modules for the gate-collector capacitance (Cgc). Please refer to Figure 15 below to observe Cgc results from channel A (blue) and channel B (orange).

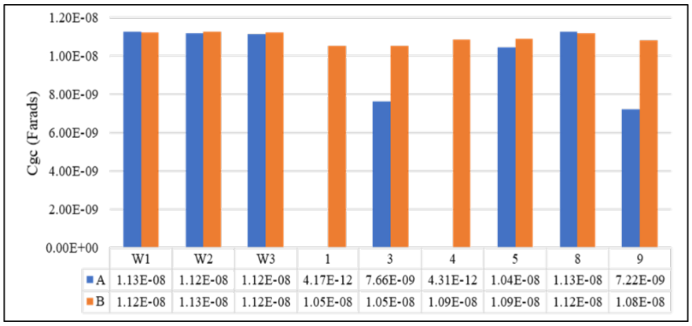

FIGURE 15: SETUP OF CURVE TRACER CONNECTED TO A POWER MODULE FOR ELECTRICAL CHARACTERIZATION.

The results obtained from the curve tracer indicate a significant change (in modules 3 and 9) or absence (in modules 1 and 4) of electrical response from some of the power modules, especially on channel A (Blue). Upon visual inspection, it was possible to observe degradation on some of the wirebonds in these modules. Based on the electrical characterization results and imaging inspection, a correlation was found between modules exhibiting lower Cgc and degradation observed in the wirebonds. The health of the wirebonds was classified into three categories: Healthy (no damage), Medium damage (i.e. crack observed), and Full damage (i.e. wirebond heel fracture detected) (see figure 16 below).

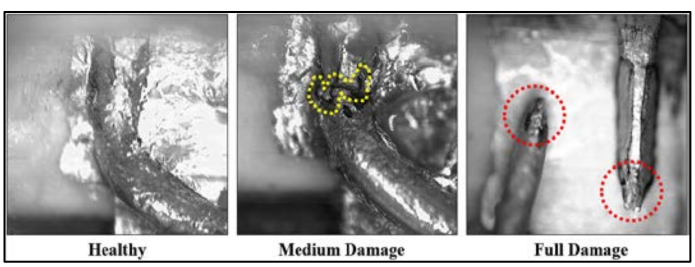

FIGURE 16: WIREBOND DEGRADATION CATEGORIZATION BASED ON IMAGING INSPECTION AND ELECTRICAL CHARACTERIZATION.

It was clear that modules with wirebond degradation had a lower Cgc, whereas modules with no damage had no significant change. Modules 1, and 4, channel A, showed full damage in wirebond, whereas modules 3, and 9, channel A, showed medium damage in wirebond. Other modules did not show wirebond damage.

4. SUMMARY

This paper discussed the degradation of IGBTs caused by accelerated thermal cycling. The modules did not show the expected increase in V_{CE} with time due to progressive die attach fatigue, thereby limiting the ability to use this signal for predicting imminent failure. Instead, failure was observed as a sudden increase in V_{CE}, which was revealed to be due to wirebond heel fracture and the major failure mechanism was thus wirebond fatigue due to thermomechanical stress caused by thermal cycling. Electrical characterization and imaging analysis helped verified wirebond damage and allowed categorizing wirebond degradation into healthy (no damage), medium damage (i.e. crack observed) and full damage (i.e. wirebond heel fracture). Based on the results from the study, wirebond damage seem to precede any other type of failure in the modules and was detectable using Cgc. This study will enable further research into prognostics analysis of wirebond failures in power electronic modules.

ACKNOWLEDGEMENTS

The authors of this paper would like to thank the members of the Center for Advanced Life Cycle Engineering (CALCE) at the University of Maryland for their support to this work. Special thanks to the National Renewable Energy Laboratory (NREL) for their collaboration and funding of this project. The authors would also like to thank Charis Smith for her technical assistance during measurements and electrical characterization of wirebonds for power modules.

REFERENCES

[1] E. Santi, S. Eskandari, B. Tian, and K. Peng, “6 - Power Electronic Modules,” in *Power Electronics Handbook (Fourth Edition)*, M. H. Rashid, Ed. Butterworth-Heinemann, 2018, pp. 157–173.

[2] S. Yang, D. Xiang, A. T. Bryant, P. Mawby, L. Ran, and P. J. Tavner, “Condition Monitoring for Device Reliability in Power Electronic Converters: A Review,” *Power Electron. IEEE Trans. On*, vol. 25, pp. 2734–2752, Dec. 2010.

[3] J. Lutz, Ed., *Semiconductor power devices: physics, characteristics, reliability*. Berlin: Springer-Verlag, 2011.

[4] V. Smet *et al.*, “Ageing and Failure Modes of IGBT Modules in High-Temperature Power Cycling,” *IEEE Trans. Ind. Electron.*, vol. 58, no. 10, pp. 4931–4941, Oct. 2011.

[5] A. Morozumi, K. Yamada, T. Miyasaka, S. Sumi, and Y. Seki, “Reliability of power cycling for igbt power semiconductor modules,” *IEEE Trans. Ind. Appl.*, vol. 39, no. 3, pp. 665–671, May 2003.

[6] X. Perpiñà *et al.*, “IGBT module failure analysis in railway applications,” *Microelectron. Reliab.*, vol. 48, no. 8, pp. 1427–1431, Aug. 2008.

[7] M. BOUARROUDJ, Z. Khatir, J. P. OUSTEN, F. BADEL, L. DUPONT, and S. Lefebvre, “Degradation behavior of 600V-200A IGBT modules under Power cycling and high temperature environment conditions,” in *18th European Symposium on Reliability of Electron Devices, Failure Physics and Analysis*, BORDEAUX, France, 2007, vol. 47, pp. 1719–1724.

[8] H. Oh, B. Han, P. McCluskey, C. Han, and B. D. Youn, “Physics-of-Failure, Condition Monitoring, and Prognostics of Insulated Gate Bipolar Transistor Modules: A Review,” *IEEE Trans. Power Electron.*, vol. 30, no. 5, pp. 2413–2426, May 2015.

[9] S. Manoharan, N. M. J. Li, C. Patel, S. Hunter, and P. McCluskey, “Mechanics of Copper Wire Bond Failure due to Thermal Fatigue,” in *2018 IEEE 20th Electronics Packaging Technology Conference (EPTC)*, 2018, pp. 874–881.

[10] W. Kexin, D. Mingxing, X. Linlin, and L. Jian, “Study of Bonding Wire Failure Effects on External Measurable Signals of IGBT Module,” *IEEE Trans. Device Mater. Reliab.*, vol. 14, no. 1, pp. 83–89, Mar. 2014.